PERGAMON

International Journal of Heat and Mass Transfer 44 (2001) 4391–4400

International Journal of HEAT and MASS TRANSFER

www.elsevier.com/locate/ijhmt

Effects of internal heat transfer and preferential diffusion on stretched spray flames

Shuhn-Shyurng Hou [a,*], Ta-Hui Lin [b]

[a] Department of Mechanical Engineering, Kun Shan University of Technology, Tainan 71003, Taiwan, ROC
[b] Department of Mechanical Engineering, National Cheng Kung University, Tainan 70101, Taiwan, ROC

Received 19 September 2000; received in revised form 8 March 2001

Abstract

The extinction of dilute spray flames propagating in a stagnation-point flow under the influence of flow stretch, preferential diffusion, and internal heat transfer is analyzed using activation energy asymptotics. A completely prevaporized mode and a partially prevaporized mode of flame propagation are identified. The internal heat transfer, associated with the liquid fuel loading and the initial droplet size of the spray, provides heat loss and heat gain for rich and lean sprays, respectively. It is found that the flow stretch coupled with Lewis number (Le) reduces and enhances the burning intensity of the lean methanol-spray flame ($Le > 1$) and rich methanol-spray flame ($Le < 1$), respectively; and that the flame extinction characterized by a C-shaped curve for the $Le > 1$ flame is dominated by the flow stretch, while the S-shaped extinction curve for the $Le < 1$ flame is mainly influenced by the internal heat loss associated with the droplet gasification process.

Keywords: Flame extinction; Dilute spray; Lewis number; Flow stretch; Stagnation-point flows

1. Introduction

A homogeneous laminar premixed flame influenced by external heat loss can be characterized by a C-shaped extinction curve (a double-valued function) [1–3]. For positively stretched flames in the stagnation-point flow, the burning intensity is weakened or intensified when the Lewis number is greater or less than one, respectively [4–7]. Here the Lewis number designates the ratio of thermal-to-mass diffusivities of the deficient reactant in the mixture. Regardless of downstream heat loss through the wall and incomplete reaction, a sufficiently large stretch can lead to the occurrence of extinction for $Le > 1$ flame, while no extinction occurs for $Le < 1$ flame.

The above descriptions were focused on the flame extinction of homogeneous mixtures caused by the external heat loss [1–3] and flow stretch [4–7] separately. However, the participation of fuel spray effects [8] further produced so-called internal heat loss (or gain), and therefore resulted in the S-shaped extinction curve (a triple-valued function) that is distinct from the C-shaped extinction one. The interaction between external and internal heat transfers on extinction of dilute spray flames has been analyzed by a series of theoretical studies in one-dimensional models [9–11]. Depending on the balance between internal and external heat transfers, dilute spray flames were characterized by a C-shaped extinction curve or a curve bounded by blow-off and flashback in the excess enthalpy theory of spray deflagration [11]. In the theoretical studies [9–11], however, the effects of flow stretch and nonunity Lewis number on the flame extinction of dilute sprays were not examined.

Subsequently, the extinction of a methane–air premixed flame propagating in a stagnation-point flow (a two-dimensional model) under the influence of an inert (water) spray has been studied by Liu et al. [12]. It was concluded that the application of the inert spray to the $Le < 1$ flame indicates that extinction characterized by an S-shaped curve is possible. In contrast, the $Le > 1$ flame can be extinguished with and without the

* Corresponding author. Tel.: +886-6-272-4833; fax: +886-6-273-4240.
E-mail address: sshou@mail.ksut.edu.tw (S.-S. Hou).

0017-9310/01/$ - see front matter
PII: S0017-9310(01)00100-4

Nomenclature

Dimensional quantities

A'	cross-sectional area of the stream
B'	preexponential factor
C'_{PG}	specific heat of the gaseous mixture
C'_{PL}	specific heat of the liquid
D'	mass diffusion coefficient
Ea'	activation energy
L'	separation distance (Fig. 1)
ℓ'_D	thickness of the diffusion zone
$\tilde{M}'$	average molar mass
n'	number density
Q'	heat of combustion per unit mass of gaseous fuel
$\tilde{R}$	universal gas constant
r'	droplet radius
S^0_L	one-dimensional adiabatic flame speed

Nondimensional quantities

$\bar{A}$	Eq. (8)
C	parameter governed by Eq. (28)
F	$F(T, Y_O) = \ln[1 + (T - T_b)/h_{LG}]$ for the vaporizing droplet or $F(T, Y_O) = \ln[1 + (T - T_b + Y_O Q)/h_{LG}]$ for the burning droplet
f_F	$f_F = 1$ and 0 for the vaporizing droplet and the burning droplet, respectively
f_O	$f_O = 0$ and -1 for the vaporizing droplet and the burning droplet, respectively
f_T	$f_T = -h_{LG}$ and $(Q - h_{LG})$ for the vaporizing droplet and the burning droplet, respectively
h_{LG}	latent heat of vaporization, $h'_{LG}/(C'_{PG}T'_i)$
Le	Lewis number, $\lambda'/(\rho'_G C'_{PG} D'_j)$
$\dot{m}$	axial mass flux $(\rho u), \rho' u'/(\rho'_i S^0_L)$
P	pressure, P'/P'_i
Pr	Prandtl number
Q	heat combustion of fuel, $Q'/(C'_{PG}T'_i)$
T	temperature, T'/T'_i
T_a	activation temperature, $Ea'/(\tilde{R}T'_i)$
T_{ad}	adiabatic flame temperature, T'_{ad}/T'_i
U	axial velocity at the burner exit, u'_i/S^0_L
u, v	axial and radial velocities, $u = u'/S^0_L$, $v = v'/S^0_L$
W	Eq. (9)
x, y	axial and radial coordinates, $x = x'/L'$, $y = y'/L'$
Y	mass fraction, $Y_F = Y'_F$, $Y_O = Y'_O/\sigma$
z	density ratio, ρ'_G/ρ'

Greek symbols

α	$\alpha = 1$ and $\alpha = 0$ for lean and rich sprays
β	mass fraction perturbation in the reaction zone
γ	$(1 - z_i)/\delta$
δ	small expansion parameter, ℓ'_D/L'
ε	small expansion parameter, $T'_{ad}\tilde{R}/Ea'$
η	stretch variable of the reaction zone, ξ/ε
θ	temperature perturbation in the reaction zone
Λ	Eq. (19)
λ'	thermal conductivity
ξ	stretch variable for the diffusion zone, $(x - x_f)/\delta$
ρ'	density
σ	stoichiometric ratio
ϕ	equivalence ratio

Superscripts

+	downstream near the flame
′	dimensional quantities

Subscripts

b	boiling state
c	droplet size for completing vaporization just at the flame front
e	state at which droplet is completely gasified
F, O	fuel and oxygen
f	flame front
G, L	gas and liquid phases
i	state at the exit plane of the burner
j	$j =$ F or O
k	$k =$ F or O in lean and rich mixtures, respectively
s	spray
w	state at wall
0, 1	zeroth- and first-order solutions

participation of the inert spray. Flow stretch and inert spray are responsible for extinction of the $Le > 1$ flame identified by a C-shaped curve and a W-shaped curve, respectively. Unfortunately, this study did not include the possible existence of fuel sprays that provide the internal heat gain associated with the secondary gasified fuel from the droplet gasification process for enhancing premixed burning under lean-spray conditions [13].

In the present study, we have formulated an extinction theory on stretched spray flames with nonunity Lewis number in a nonconserved system in which the initial gas-phase composition is maintained the same, but the liquid fuel loading is systematically varied. Therefore, the influences of liquid fuel will be independently explored without the participation of the leaning effect from the gas-phase mixture. Furthermore, the coupling effects of flow stretch and internal heat transfer on extinction and flashback of stretched spray flames with nonunity Lewis number will be emphasized.

We consider a steady, planar, premixed flame generated in a stagnation-point, two-phase flow in which the dispersed phase is simulated by a monodisperse, dilute and chemical reactive spray. The purpose of this

study is to investigate flame extinction and flame flashback under the influences of Lewis number, flow stretch, and internal heat transfer that is a function of liquid fuel loading and liquid fuel droplet size. We shall also restrict our analysis to dilute sprays, so that the amount of liquid fuel loading in the fresh mixture is very small and can be expanded in perturbation analysis.

2. Formulation

Fig. 1 shows the schematic of the stagnation-point configuration considered here in which a two-phase premixture of gaseous fuel, air and liquid fuel droplets impinges onto a wall that is adiabatic and impermeable. The injection velocity at the burner exit is assumed to be uniform and is denoted by a nondimensional value, U. The cylindrical coordinates (x, y) with the origin at the center of the wall are nondimensionalized by the separation distance (L') between the burner and the wall. The locations of the burner exit and the premixed flame are respectively denoted by 1 and x_f. A completely prevaporized mode ($r'_i \leqslant r'_c$) and a partially prevaporized mode ($r'_i > r'_c$) are identified by a critical initial droplet size (r'_c) for the droplet to achieve complete evaporation at the premixed flame front [14]. The initial droplet temperature is constant and assumed to be the same as the inflowing gas temperature. We assume that the droplet will start to evaporate only when the gas temperature has reached the boiling point of the liquid. Droplets then ignite upon crossing the flame, and vanish at $x = x_e$ upon complete combustion for lean sprays or complete evaporation for rich sprays. The gaseous mixture in each section is homogeneous due to instantaneous mixing of the initial gasified reactants, vaporized fuel and products [14,15].

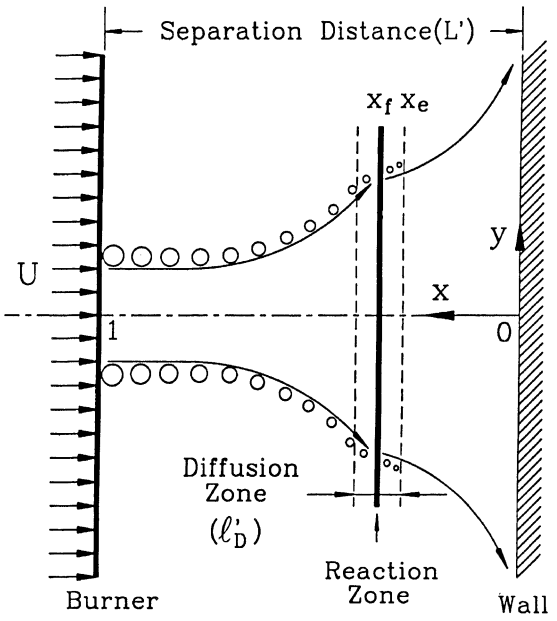

Fig. 1. Schematic diagram of a premixed flame propagating in a stagnation-point flow under the influence of combustible sprays.

A small parameter $\delta = \ell'_D/L' \ll 1$ based on large activation energy asymptotics is simply assumed, where $\ell'_D = \lambda'/(\rho'_{Gi} C'_{PG} S^0_L)$ indicates the thickness of the diffusion zone; here λ' is the thermal conductivity, C'_{PG} is the specific heat at constant pressure, ρ'_{Gi} is the density of fresh gas at the burner exit and S^0_L is the one-dimensional adiabatic laminar flame speed of a premixed flame. Due to the fast chemical reaction, a thinner reaction zone is assumed to be embedded within the diffusion zone, as shown in Fig. 1. The amount of liquid loading is assumed to be $O(\varepsilon)$ of the total mixture mass because the spray is dilute and monodisperse. We assume no interaction between droplets during their lifetime. Here the small parameter of expansion, ε, is the ratio of thermal energy to large activation energy in the combustion process. In the analysis, small parameters δ and ε are assumed to be of the same order for the matching of the reaction zone [13]. By assuming the extent of spray heterogeneity as $O(\varepsilon)$, we are excluding phenomena related to the dense spray region near the nozzle exit, where most of the fuel is still in liquid form while very little air has been entrained [14].

To suppress interactions between droplets and the gas flow or between droplets and the wall, the droplet size must be small enough, and its motion in phase with that of the gas [12]. Therefore, droplets with a selected size can penetrate into the premixed flame, but almost achieve complete evaporation in passing through the diffusion zone. This consideration will narrow down the applicable range of droplet size herein. However, the influence of the droplet size on flame extinction can still be apparent to us. No slip is assumed for mathematical simplicity and thus clarity in understanding the phenomena of interest. This assumption is also consistent with the dilute spray assumption applicable to regions far away from the injection nozzle, where the initial gas-droplet velocity disparity due to injection has been largely reduced through drag [14,15].

Furthermore, moderate rates of flow stretch allowing the flame to sit outside the viscous boundary layer are considered. Finally, we assume that the fuel and oxidizer reaction for the bulk premixed flame is one-step overall, that the droplet gasification follows the d^2-law, and that constant property simplifications apply. More detailed assumptions and comments were generally illustrated in earlier studies [12,13].

The total number of droplets crossing any plane normal to the central axis per second is set to be con-

stant, for a given stream tube of axisymmetrical stagnation-point flow

$$n'u'A' = n'_{\mathrm{i}}u'_{\mathrm{i}}A'_{\mathrm{i}}, \tag{1}$$

where A' is the cross-sectional area of the stream tube, n' is the number density and u' is the axial velocity. Following Williams [15], we designate the extent of gas-phase heterogeneity by the variable $z = \rho'_{\mathrm{G}}/\rho'$ where ρ' is the overall density of the two-phase mixture, and $\rho' = \rho'_{\mathrm{G}} + \rho'_{\mathrm{S}}$, in which $\rho'_{\mathrm{S}} = (4/3)\pi(r'_{\mathrm{i}})^3 n'\rho'_{\mathrm{L}}$ shows the spray density. Note that $z = 1$ represents the completely vaporized state. In the formulation, variables are nondimensionalized by their values at the exit plane of the burner, except that the characteristic velocity for nondimensionalization is S^0_{L} such that $U = u'/S^0_{\mathrm{L}}$. Quantities with and without primes are dimensional and nondimensional, respectively.

Therefore, the nondimensional equations for overall continuity, gas-phase continuity, conservations of fuel, oxidizer, energy, and momentum, respectively, are given by

$$\frac{\partial}{\partial x}(\rho u) + \frac{1}{y}\frac{\partial}{\partial y}(y\rho v) = 0, \tag{2}$$

$$\frac{\partial}{\partial x}(\rho z u) + \frac{1}{y}\frac{\partial}{\partial y}(y\rho z v) = \delta^{-1}\bar{A}(1-z)^{1/3} \times (1-z_{\mathrm{i}})^{2/3}F(T, Y_{\mathrm{O}})/(zT), \tag{3}$$

$$\frac{\partial}{\partial x}(\rho z u Y_j) + \frac{1}{y}\frac{\partial}{\partial y}(y\rho z v Y_j) - \delta Le_j^{-1}\left[\frac{\partial^2 Y_j}{\partial x^2} + \frac{1}{y}\frac{\partial}{\partial y}\left(y\frac{\partial Y_j}{\partial y}\right)\right] = \delta^{-1}W + f_j\left[\frac{\partial}{\partial x}(\rho z u) + \frac{1}{y}\frac{\partial}{\partial y}(y\rho z v)\right], \quad j = \mathrm{F}, \mathrm{O}, \tag{4}$$

$$\frac{\partial}{\partial x}(\rho z u T) + \frac{1}{y}\frac{\partial}{\partial y}(y\rho z v T) - \delta\left[\frac{\partial^2 T}{\partial x^2} + \frac{1}{y}\frac{\partial}{\partial y}\left(y\frac{\partial T}{\partial y}\right)\right] = -\delta^{-1}WQ + f_{\mathrm{T}}\left[\frac{\partial}{\partial x}(\rho z u) + \frac{1}{y}\frac{\partial}{\partial y}(y\rho z v)\right], \tag{5}$$

$$\rho\left(u\frac{\partial u}{\partial x} + v\frac{\partial u}{\partial y}\right) = -\bar{P}\frac{\partial P}{\partial x} + \delta Pr\left[\frac{\partial^2 u}{\partial x^2} + \frac{1}{y}\frac{\partial}{\partial y}\left(y\frac{\partial u}{\partial y}\right)\right], \tag{6}$$

$$\rho\left(u\frac{\partial v}{\partial x} + v\frac{\partial v}{\partial y}\right) = -\bar{P}\frac{\partial P}{\partial y} + \delta Pr\left[\frac{\partial^2 v}{\partial x^2} + \frac{\partial}{\partial y}\left(\frac{1}{y}\frac{\partial}{\partial y}(yv)\right)\right], \tag{7}$$

where

$$\bar{P} = P'_{\mathrm{i}}/\left[\rho'_{\mathrm{i}}(S^0_{\mathrm{L}})^2\right], \qquad \bar{A} = 3\ell'^2_{\mathrm{D}}P'\bar{\tilde{M}}'/\left[T'_{\mathrm{i}}\rho'_{\mathrm{L}}\tilde{R}(r'_{\mathrm{i}})^2\right], \tag{8}$$

and

$$W = -\left(B'\sigma/\bar{\tilde{M}}'_{\mathrm{O}}\right)\left(P'\bar{\tilde{M}}'/\tilde{R}\right)^2\left\{\lambda'/[C'_{PG}(\rho'_{\mathrm{i}}S^0_{\mathrm{L}})^2]\right\}Y_{\mathrm{F}}Y_{\mathrm{O}} \times \exp(-T_{\mathrm{a}}/T). \tag{9}$$

In the above equations, $Q = Q'/(C'_{PG}T'_{\mathrm{i}})$ and $h_{\mathrm{LG}} = h'_{\mathrm{LG}}/(C'_{PG}T'_{\mathrm{i}})$ represent the heat of combustion per unit mass of gaseous fuel and the latent heat of vaporization for the liquid fuel, respectively. In Eqs. (3)–(5), $F(T, Y_{\mathrm{O}})$, f_{F}, f_{O}, and f_{T} are given by $\ln[1 + (T - T_{\mathrm{b}})/h_{\mathrm{LG}}]$, 1, 0, and $-h_{\mathrm{LG}}$ for the vaporizing droplet and $\ln[1 + (T - T_{\mathrm{b}} + Y_{\mathrm{O}}Q)/h_{\mathrm{LG}}]$, 0, −1, and $(Q - h_{\mathrm{LG}})$ for the burning droplet, respectively. Finally, the ideal gas equation and the conservation of mass flux for the axisymmetric stream tube are applied to the deviation of the gas-phase continuity.

The boundary conditions at the burner exit, $x = 1$, are specified as $u = U$, $v = 0$, $p = p_{\mathrm{i}}$, $Y_j = Y_{j\mathrm{i}}$, $T = T_{\mathrm{i}}$, and $z = z_{\mathrm{i}}$. Since the premixed flame always stays outside of the viscous boundary layer which provides an $\mathrm{O}(\delta^{1/2})$ thick displacement for the outer flow, the boundary conditions at $x = 0$ can be adequately given by $u = 0$, $z = 1$, $Y_j = Y_{j\mathrm{w}}$, and $T = T_{\mathrm{w}}$. The problem will be solved performing the separate analysis on three regions, namely the diffusion zone, the reaction zone and the outer hydrodynamic zone. Based on the assumption of δ and ε being the same order, the stretched variables are given by $\xi = (x - x_{\mathrm{f}})/\delta$ and $\eta = \xi/\varepsilon$ for the diffusion zone and the reaction zone, respectively.

3. The diffusion zone

In the diffusion zone, the dependent variables are expanded with respect to the small parameter of δ as

$$\begin{aligned} T &= T_0 + \delta T_1 + \mathrm{O}(\delta^2), \\ Y_j &= Y_{j0} + \delta Y_{j1} + \mathrm{O}(\delta^2), \quad j = \mathrm{F}, \mathrm{O}, \\ u &= u_0 + \delta u_1 + \mathrm{O}(\delta^2), \\ v &= v_0 + \delta v_1 + \mathrm{O}(\delta^2), \\ \rho &= \rho_0 + \delta\rho_1 + \mathrm{O}(\delta^2). \end{aligned} \tag{10}$$

In order to satisfy the flame structure, z is also expanded as

$$z = 1 - \delta\gamma z_0 + \mathrm{O}(\delta^2) \tag{11}$$

such that $z_{\mathrm{i}} = 1 - \delta\gamma$ for a dilute spray. The liquid loading will be characterized by the parameter γ. Substituting Eq. (10) into Eqs. (2), (4) and (5) and expanding, we have

$$\frac{\partial}{\partial\xi}(\rho_0 u_0) = \frac{\partial}{\partial\xi}(\dot{m}_0) = 0,$$
$$\dot{m}_0\frac{\partial Y_{j0}}{\partial\xi} - \frac{1}{Le_j}\frac{\partial^2 Y_{j0}}{\partial\xi^2} = 0, \quad j = \mathrm{F},\mathrm{O}, \tag{12}$$
$$\dot{m}_0\frac{\partial T_0}{\partial\xi} - \frac{\partial^2 T_0}{\partial\xi^2} = 0,$$

from which the zeroth-order solutions are readily determined to be

$$Y_{j0} = \begin{cases} Y_{j,\mathrm{i}} - Y_{k,\mathrm{i}}\,\mathrm{e}^{\dot{m}_0 Le_j\xi}, & j = \mathrm{F},\mathrm{O}, \quad \xi < 0, \\ Y_{j,\mathrm{i}} - Y_{k,\mathrm{i}} & \xi > 0, \end{cases} \tag{13}$$

and

$$T_0 = \begin{cases} 1 + (T_{\mathrm{ad}} - 1)\mathrm{e}^{\dot{m}_0\xi}, & \xi < 0, \\ T_{\mathrm{ad}}, & \xi > 0, \end{cases} \tag{14}$$

where $k = \mathrm{F}$ and $k = \mathrm{O}$ for lean and rich mixtures, respectively. $\dot{m}_0$ is a constant and denotes the axial mass flux normalized by the adiabatic premixed value, $\rho_{\mathrm{i}}' S_{\mathrm{L}}^0$.

Using Eqs. (11) and (14), we obtain

$$z_0 = \left\{1 - \frac{2\bar{A}}{3\dot{m}_0}\int_{\xi_v}^{\xi}\left[1 + (T_{\mathrm{ad}} - 1)\mathrm{e}^{\dot{m}_0\xi}\right]^{-1} \ln\left[1 + \frac{(1 - T_{\mathrm{b}}) + (T_{\mathrm{ad}} - 1)\mathrm{e}^{\dot{m}_0\xi}}{h_{\mathrm{LG}}}\right]\mathrm{d}\xi\right\}^{3/2}, \quad \xi < 0, \tag{15}$$

from Eq. (3), while the position (ξ_v) for the initiation of droplet evaporation is given by

$$\xi_v = \frac{1}{\dot{m}_0}\ln\left(\frac{T_{\mathrm{b}} - 1}{T_{\mathrm{ad}} - 1}\right). \tag{16}$$

4. The reaction zone

In the reaction zone of the bulk gas-phase flame, the solution is expanded around the flame-sheet limit as

$$T = T_{\mathrm{ad}} + \varepsilon T_{\mathrm{ad}}\theta + \mathrm{O}(\varepsilon^2),$$
$$Y_j = Y_{j\mathrm{f}} + \varepsilon\beta_j + \mathrm{O}(\varepsilon^2), \quad j = \mathrm{F},\mathrm{O}, \tag{17}$$

to result in

$$Le_j^{-1}\frac{\mathrm{d}^2\beta_j}{\mathrm{d}^2\eta^2} = -T_{\mathrm{ad}}\frac{\mathrm{d}^2\theta}{\mathrm{d}\eta^2} = \frac{\Lambda}{2}Q\left(\frac{T_{\mathrm{ad}}}{T_{\mathrm{a}}}\right)(Y_{\mathrm{Ff}} + \varepsilon\beta_{\mathrm{F}})(Y_{\mathrm{Of}} + \varepsilon\beta_{\mathrm{O}})\exp\theta, \tag{18}$$

where

$$\Lambda = 2\left(\frac{T_{\mathrm{ad}}}{T_{\mathrm{a}}}\right)\left(\frac{B'\sigma}{\bar{\tilde{M}}_{\mathrm{O}}'}\right)\left(\frac{p'\bar{\tilde{M}}'}{\tilde{R}}\right)^2\left[\frac{\lambda'}{C_{PG}'(\rho_{\mathrm{i}}' S_{\mathrm{L}}^0)^2}\right] \times \exp\left(-\frac{T_{\mathrm{a}}}{T_{\mathrm{ad}}}\right), \tag{19}$$

is the flame speed eigenvalue. By using the local Shvab–Zeldovish formulation and the matching conditions at $\eta \to \pm\infty$ [14], we have

$$\dot{m}_0^2 = \exp[T_1(0^+)/T_{\mathrm{ad}}], \tag{20}$$

in which the first-order temperature, $T_1(0^+)$, denotes the $\mathrm{O}(\delta)$ downstream temperature perturbation at the flame. Eq. (20) shows that the flame propagation flux ($\dot{m}_0$) is exponentially affected by the first-order temperature downstream near the flame. Adding Eq. (4) to Eq. (5), and then integrating it from $\xi = -\infty$ to $\xi = 0^+$ leads to

$$T_1(0^+) = \gamma\bar{D} - \frac{\bar{K}\Gamma}{\dot{m}_0^2} \tag{21}$$

in which

$$\Gamma = QY_{j\mathrm{i}}\int_0^1 [1 - \tilde{\omega}^{(Le_j - 1)}]/(1 + \tilde{\omega}QY_{j\mathrm{i}})d\tilde{\omega}$$

represents the Lewis number effect, and $\bar{K} = (1/y)(\partial/\partial y)(yv)$ shows the flow stretch. The spray effect including the liquid fuel loading and the initial droplet size comes from $\gamma\bar{D}$ in Eq. (21), where

$$\bar{D} = \left[T_{\mathrm{b}} - \frac{C_{PL}'}{C_{PG}'}(T_{\mathrm{b}} - 1)\right] - (T_{\mathrm{ad}} + h_{\mathrm{LG}} - \alpha Q) \times \left(1 - \dot{m}_0\int_0^{\xi_{\mathrm{e}}} z_0\,\mathrm{e}^{-\dot{m}_0\xi}\mathrm{d}\xi\right), \tag{22}$$

and

$$\xi_{\mathrm{e}} = z_0(0)^{2/3}/\{2\bar{A}\ln[1 + (T_{\mathrm{ad}} - T_{\mathrm{b}} + \alpha QY_{j\mathrm{w}})/h_{\mathrm{LG}}]/3\dot{m}_0 T_{\mathrm{ad}}\}, \tag{23}$$

showing the vaporized state. Here, $\alpha = 1$ and $\alpha = 0$ for lean and rich sprays, respectively. The liquid fuel loading is represented by γ through the expansion of $z_{\mathrm{i}} = 1 - \delta\gamma$ [13]. A larger value of γ means that the dilute spray has a relatively larger amount of liquid fuel. For the case of completely prevaporized sprays, Eq. (22) is simplified to be

$$\bar{D} = \left[T_{\mathrm{b}} - \frac{C_{PL}'}{C_{PG}'}(T_{\mathrm{b}} - 1)\right] - (T_{\mathrm{ad}} + h_{\mathrm{LG}} - \alpha Q), \tag{24}$$

indicating that there is no contribution on $T_1(0)^+$ coming from the droplet size.

5. The hydrodynamic zone

The flow stretch, shown in Eq. (21), and the flame position will be determined by solving the flow field of the outer hydrodynamic zone. Since the flame sits outside of the boundary layer and $\delta \to 0$, we neglect the flow viscosity and only consider the zeroth-order solutions which are governed by Eqs. (2), (6) and (7) with

boundary conditions being $u(1) = -U$, $u(0) = v(1) = 0$. The flow density on either side of the flame is given by

$$\rho = \begin{cases} 1, & x > x_f, \\ \rho_w = \rho'_w/\rho'_i, & x < x_f. \end{cases} \tag{25}$$

Since the spray effect is being $O(\varepsilon)$, jump conditions for the leading order across the flame follow the Rankine–Hugoniot relations [3].

The governing equations admit a self-similar solution of the form

$$u = 2F(x) \quad \text{and} \quad v = -y\frac{d}{dx}F(x). \tag{26}$$

Following the standard procedure used in Kim and Matalon [4] and Tien and Matalon [16], the flow field of the unburnt side of the flame can be found as

$$\begin{aligned} u &= C(x-1)^2 + U(x-2)x, \\ v &= -y(C+U)(x-1), \end{aligned} \tag{27}$$

where C is a parameter determined by the following equation:

$$\frac{1}{2}\rho_w(x_f-1)^2\left[\frac{(x_f-1)}{\rho_w} - x_f\right]^2 (C+U)^2 + \frac{1}{2}U(C+U) \times \left[x_f(x_f-2) - 2\frac{(x_f-1)^2}{\rho_w}\right] + \frac{1}{2}\frac{U^2}{\rho_w} = 0. \tag{28}$$

For the flow stretch, we find

$$\frac{1}{y}\frac{\partial}{\partial y}(yv) = -2(C+U)(x-1), \quad x > x_f. \tag{29}$$

Since $\dot{m}_0 = 1u(x_f)$ near the upstream side of the flame, the flame position should be finally identified by the coupling of Eqs. (20), (21), and (27)–(29).

Sample calculations based on Eqs. (20)–(24) and (27)–(29) on $\dot{m}_0$ and x_f for methanol burning in air are now considered in a nonconserved manner in which the initial gas-phase composition is fixed, i.e., Φ_G is maintained constant, but the liquid fuel loading is systematically varied. Therefore, the influences of liquid fuel will be independently explored without the participation of the leaning effect from the gas-phase mixture. The influences of flow stretch and preferential diffusion on dilute spray flames in the problem will be assessed based on four parameters, namely the initial droplet radius (r'_i), the liquid fuel loading (γ), flow stretch ($\bar{K}$), and Lewis number (Le). Here r'_i and γ show the internal heat transfer (heat gain or heat loss) for the fuel spray. We use U instead of $\bar{K}$ as a measurable variable to represent flow stretch in the problem because there is a linear relationship between U and $\bar{K}$ [12]. Lewis number is defined as $\lambda'/(\rho'_G C'_{PG} D'_j)$ in which the diffusion coefficient of the deficient reactant in the mixture is used and variables are determined based on the mean gaseous temperature upstream of the flame. Methanol–air premixture of $\Phi_G = 0.8$ and $\Phi_G = 1.5$, corresponding to $Le = 1.0371$ and 0.9477, respectively, are adopted to show the influence of nonunity Lewis number.

6. Lean spray flames with $Le > 1$

Considering the effects of the liquid fuel loading, the interaction between the internal heat transfer associated with liquid droplets evaporation and the flow stretch on the dilute spray flames is first examined by investigating the prevaporized sprays ($r'_i \leqslant r'_c$) in which no liquid droplet exists downstream of the flame. Fig. 2 shows the flame propagation flux ($\dot{m}_0$) and the flame position (x_f) of lean methanol-spray flames as functions of U and γ under completely prevaporized conditions ($r'_i \leqslant r'_c$). Since the flame in stagnation-point flow suffers a positive stretch, the increase of flow stretch would be expected to result in the decrease in burning intensity for $Le > 1$. Therefore, the upper and lower branches of the C-shaped extinction curves correspond to the stable and unstable solutions, respectively, and are conjoined at critical points represented by the symbol •. The critical points are identified as conditions of flame extinction. For a given γ, the increase of U first leads to decreases of both $\dot{m}_0$ and x_f indicating that a weakened flame sits closer to the wall enduring a larger flow stretch, and finally results in flame extinction when the flow stretch is large enough. This is mainly caused by the suppression of burning intensity by flow stretch for an $Le > 1$ flame. However, the decrease of U shows an opposite trend in response to the flame flux, and eventually leads to flame flashback [11,13] denoted by the symbol ■. The lean

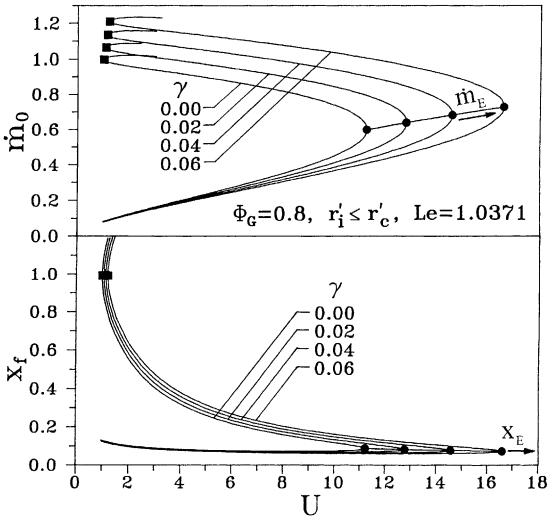

Fig. 2. Variations of the flame flux ($\dot{m}_0$) and the flame position (x_f) with the flow stretch (U) and the liquid fuel loading (γ) for lean spray flames with $Le = 1.0371$.

spray flame with the larger γ providing additional internal heat gain resulted from burning the secondary gasified fuel, will be extinguished at a larger flow stretch, as shown in Fig. 2. We understand that extinction of a lean spray flame with $Le > 1$ is mainly dominated by the external heat loss associated with the flow stretch, and is modified by the internal heat gain coming from the spray. Finally, the flammability limit identified by the distance between the maximum and minimum flow stretch is found to widen with increasing γ, for a lean spray flame with $Le > 1$.

Concerning the partially prevaporized sprays ($r'_i > r'_c$), the influence of the initial droplet size on flame characteristics is shown in Fig. 3 for a lean methanol-spray flame of $\Phi_G = 0.8$, $\gamma = 0.04$, and $Le = 1.0371$. Fig. 3 shows that with increasing initial droplet size, the upper branch corresponding to the stable solution for a partially prevaporized spray first deviates from that for the completely prevaporized spray ($r'_i \leqslant r'_c$), and approaches that for a homogeneous mixture ($\gamma = 0$). This illustrates that the flame flux decreases with increased initial droplet size or flow stretch. The former is due to the reduction of internal heat gain; the latter is caused by the augmentation of the $Le > 1$ effect. Considering the droplet gasification process for a lean spray, the liquid fuel absorbs heat for upstream prevaporization, produces the secondary gasified fuel for bulk gas-phase burning, burns through droplet combustion afterwards, and finally results in internal heat gain. A lean spray containing larger droplets with weaker prevaporization upstream of the flame provides a smaller amount of internal heat gain, and therefore has a diminished burning intensity. Hence, it can be extinguished by a smaller flow stretch. Furthermore, the extent of flammability for a lean partially prevaporized spray with $Le > 1$ decreases with increasing droplet size.

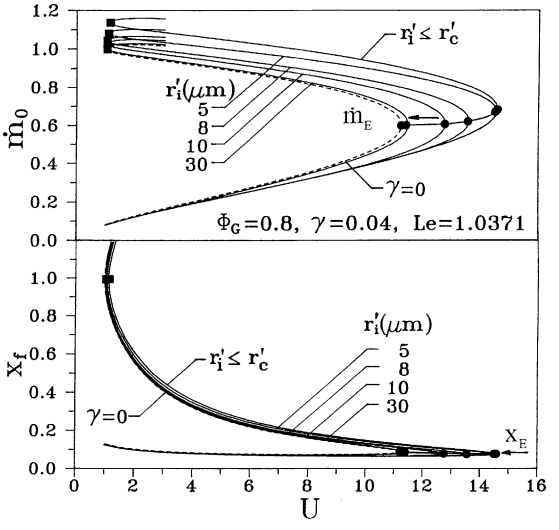

Fig. 3. Flame flux ($\dot{m}_0$) and flame position (x_f) as a function of the flow stretch (U) with various values of r'_i for a lean spray flame ($\Phi_G = 0.8$, $\gamma = 0.04$, and $Le = 1.0371$).

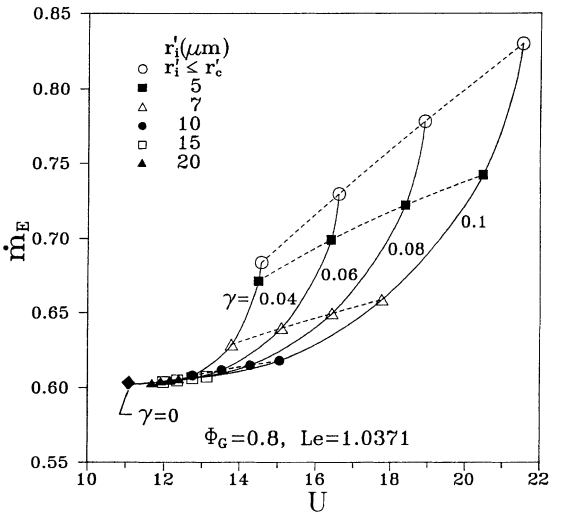

Fig. 4. The flame flux at extinction $\dot{m}_E$ as functions of the flow stretch (U) and the liquid fuel loading (γ).

The flame propagation flux at extinction, $\dot{m}_E$, as a function of U is shown in Fig. 4 for various values of r'_i and γ in lean sprays. Results show that the $\dot{m}_E$ value is decreased with increased r'_i or decreased γ, and also approaches the asymptotic value, $\exp(-0.5)$, identified as the flame flux at extinction of a homogeneous premixture according to the flame quenching theory [3]. It is expected that increasing r'_i or decreasing γ suppresses the droplet vaporization, and results in a weaker spray burning approaching to the homogeneous burning. Therefore, the value of U at extinction is also decreased with increased r'_i or decreased γ.

7. Rich spray flames with $Le < 1$

Fig. 5 shows the flame propagation flux ($\dot{m}_0$) and the flame position (x_f) of rich methanol-spray flames ($\Phi_G = 1.5$ and $Le = 0.9477$) as functions of U and γ under completely prevaporized conditions. Contrary to the lean spray, the liquid fuel absorbs heat for upstream prevaporization, producing the secondary gasified fuel which is equivalent to an inert substance with no contribution to burning for a rich spray, thus providing an overall internal heat loss, and subsequently weakening the flame propagation flux. The upper branch of the $\dot{m}_0$ curve shows stable solutions, while the lower branch of the x_f curve represents the corresponding stable solutions. From Fig. 5, the characteristic curve of $\gamma = 0$ reveals that a homogeneous flame with $Le < 1$ has a larger propagating flux and is pushed closer to the wall with

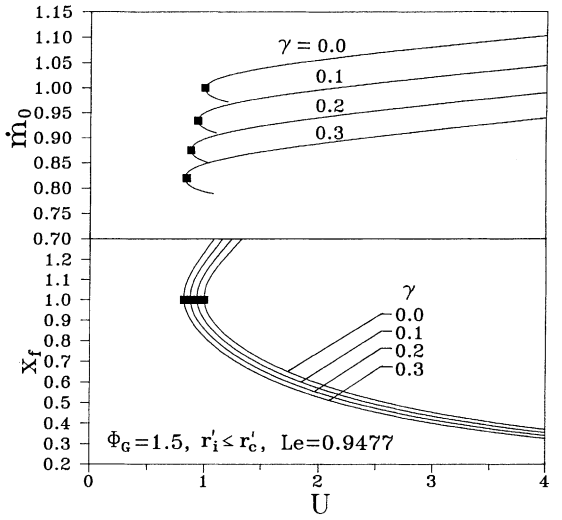

Fig. 5. Variations of the flame flux ($\dot{m}_0$) and the flame position (x_f) with the flow stretch (U) and the liquid fuel loading (γ) for rich spray flames with $Le = 0.9477$.

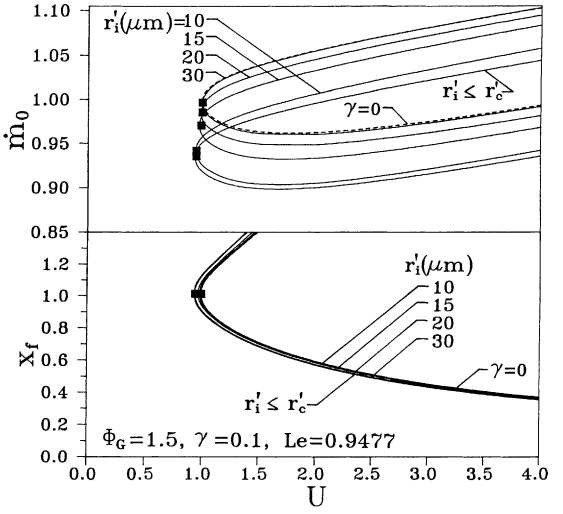

Fig. 6. Flame flux ($\dot{m}_0$) and flame position (x_f) as a function of the flow stretch (U) with various values of r_i' for a rich spray flame ($\Phi_G = 1.5$, $\gamma = 0.1$, and $Le = 0.9477$).

increases in the flow stretch. Therefore, flame flashback, rather than flame extinction, occurs for the homogeneous flame ($\gamma = 0$). For a given U, the increase of γ (the increase of the internal heat loss) leads to decreases in both $\dot{m}_0$ and x_f because a larger γ requires a larger amount of heat absorption from flame to droplets for upstream evaporation. Furthermore, it is noteworthy that the flow stretch still dominates the flame characteristics.

For partially prevaporized sprays, the response of flame flux ($\dot{m}_0$) on the flow stretch is indicated in Fig. 6, with various initial droplet sizes, for a rich methanol-spray of $\Phi_G = 1.5$, $\gamma = 0.1$, and $Le = 0.9477$. Fig. 6 also depicts that with increases in the initial droplet size, the upper branch corresponding to the stable solution for a partially prevaporized spray first deviates from that for the completely prevaporized spray ($r_i' \le r_c'$), and approaches that for a homogeneous mixture ($\gamma = 0$). It is expected that no flame extinction occurs with increasing flow stretch, if the rich sprays ($Le < 1$) consist of a smaller γ. This characteristic is caused by the smaller amount of internal heat gain and the enlarged burning intensity resulting from flow stretch for $Le < 1$ flame. Obviously, flow stretch still dominates flame characteristics in these circumstances. According to Fig. 6, it is found that the flame flux increases with increased flow stretch or enlarged initial droplet size. The former is caused by the enhancement of the $Le < 1$ effect; the latter is due to the reduction of internal heat loss. Hence, a rich methanol-spray ($Le < 1$) containing large droplets endures a weaker upstream prevaporization, provides a smaller amount of internal heat loss, and has an enhanced burning intensity. The upper branch of the $\dot{m}_0$ curve for a partially prevaporized spray containing a given value of r_i' or the completely prevaporized spray shows that the decrease of the flow stretch from a large value first leads to a monotonical decrease of the flame flux, finally resulting in flame flashback represented by the turning point. Note that flame flashback occurs at a smaller $\dot{m}_0$ when the spray has a smaller droplet size, as shown in Fig. 6.

The variations of $\dot{m}_0$ and x_f with U and r_i' for the rich methanol-spray flame with the liquid fuel loading

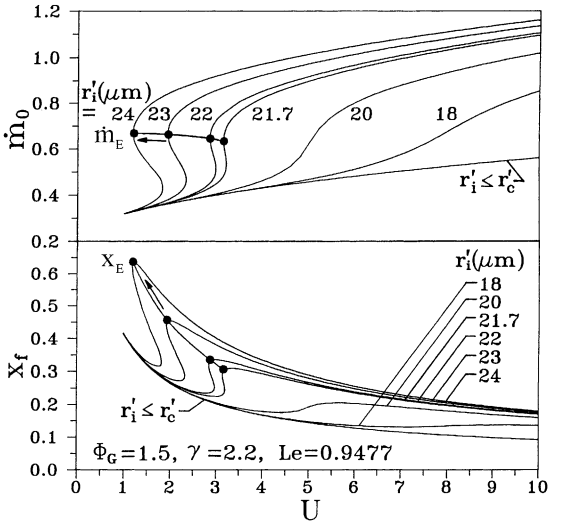

Fig. 7. Flame flux ($\dot{m}_0$) and flame position (x_f) as a function of the flow stretch (U) with various values of r_i' for a rich spray flame ($\Phi_G = 1.5$, $\gamma = 2.2$, and $Le = 0.9477$).

$\gamma = 2.2$ are indicated in Fig. 7. Results show that the flame flux (flame position) is reduced (increased) with decreasing (decreasing) the flow stretch or reducing (increasing) the initial droplet size. The former is due to the suppression of the $Le < 1$ effect, the latter is caused by the enhancement of heat loss coming from methanol vaporization. The characteristic curve of flame flux for a given value of $r_i'(r_i' < r_i'^* = 21.7\ \mu m)$ shows that by decreasing the flow stretch from a large value, the flame flux initially influenced by the partially prevaporized spray is monotonically reduced and eventually ends at the completely prevaporized condition, therefore, flame extinction does not occur. However, Fig. 7 further shows that the rich-methanol flames ($Le < 1$) enduring small flow stretch can be extinguished, if droplet sizes are large enough ($r_i' \geqslant r_i'^* = 21.7\ \mu m$). Considering a spray with a fixed amount of γ, a larger droplet size provides the flame with a smaller heat loss. Therefore, flame extinction occurs as the flame endured a smaller flow stretch. The S-shaped extinction curve (a triple-valued function) which differs from the C-shaped one (a double-valued function) points out that the flame extinction is dominated by internal heat loss under the condition of $Le < 1$ spray flames experiencing smaller flow stretch. Fig. 7 also indicates that under the influences of methanol spray and flow stretch, the $Le < 1$ spray flames can be quenched in the region far away from the wall. These interesting extinction characteristics for the $Le < 1$ flame were not found in the preliminary results [13].

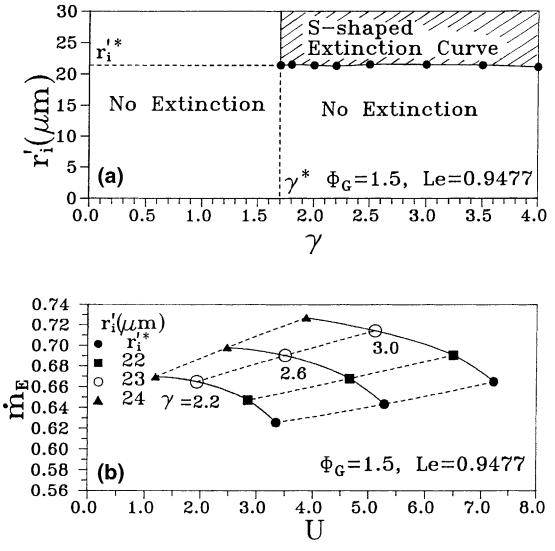

Fig. 8. (a) The map of possible burning and S-shaped extinction curves for rich sprays ($\Phi_G = 1.5$ and $Le = 0.9477$); (b) the flame flux at extinction ($\dot{m}_E$) as functions of the flow stretch (U) and the liquid fuel loading (γ).

Fig. 8(a) shows the map of possible extinction curves for rich sprays of $\Phi_G = 1.5$. For the rich-methanol spray with $Le < 1$, the S-shaped curve is found when it experiences a partially prevaporized spray with the liquid fuel loading and the droplet size large enough (in the region of $\gamma \geqslant \gamma^* = 1.7$ and $r_i' \geqslant r_i'^* = 21.7\ \mu m$). The flame propagation flux at extinction, $\dot{m}_E$, as a function of U is shown in Fig. 8(b) for various values of r_i' and γ in rich sprays. Results show that for a fixed amount of γ, the $\dot{m}_E$ and its corresponding flow stretch (U) at extinction are respectively increased and decreased with increased initial droplet radius. This characteristic is the same as that described in Fig. 7. Furthermore, for a fixed value of r_i' the $\dot{m}_E$ and its associated flow stretch at extinction are increased with increased liquid fuel loading. Considering a rich spray with a fixed value of r_i', the increase of γ results in the increase of internal heat loss because the secondary gasified fuel in a rich spray is equivalent to an inert without any contribution to burning. Hence, extinction characterized by an S-shaped curve is achieved as the flame endures a larger flow stretch.

8. Conclusions

An extinction theory of stretched premixed flames with combustible sprays was developed using activation energy asymptotics to explore the influences of liquid fuel spray, flow stretch and Lewis number on the flame extinction and flame flashback of methanol sprays. The concluding remarks are summarized as follows:

1. The internal heat transfer embedded in the rich and lean spray respectively provides heat loss and heat gain for the system. The flow stretch weakens and strengthens the burning intensity of the $Le > 1$ flame (lean methanol-flame) and the $Le < 1$ flame (rich methanol-flame), respectively.
2. For the lean methanol-spray flame with $Le > 1$, the burning strength weakened by the flow stretch can be intensified when it consists of a larger amount of liquid fuel loading or a smaller initial droplet size. However, the external heat loss associated with the flow stretch is found to strongly dominate the tendency for flame extinction.
3. For the rich methanol-spray flame with $Le < 1$, flame flashback, rather than flame extinction, exists in a completely prevaporized spray or a partially prevaporized spray having a small amount of liquid fuel loading. However, the flame extinction characterized by an S-shaped curve can occur after enduring a small flow stretch and experiencing a partially prevaporized spray composed of the large enough liquid fuel loading and sufficiently large droplet size.
4. Flame extinction characterized by a C-shaped curve for the $Le > 1$ flame is dominated by the flow stretch,

while the S-shaped extinction curve for the $Le < 1$ flame is mainly influenced by internal heat loss.

In view of the theoretical results, we realize that the understanding on flame extinction and flammability limits should be verified by the experiment, and further explored by considering a more realistic model with advanced theoretical and numerical techniques. The two-phase flow configuration considered here was first introduced by Chen et al. [17] in their experiment. The spray system is rebuilt and improved [18–20] to examine the burning characteristics of spray flames. Notably, the phenomenon of the droplets penetrating the flame surface, defined as the partially prevaporized mode in the present study, is apparent by using the enhanced spray system and the well-controlled experimental parameters. Detailed comparisons between this work and the experimental investigations [18–20] will be addressed in a separate study in the near future.

Acknowledgements

This work was supported by the National Science Council, Taiwan, ROC, under contract NSC89-EPA-Z-006-008.

References

[1] D.B. Spalding, A theory of inflammability limits and flame-quenching, Proc. R. Soc. London A240 (1957) 83–100.
[2] J.D. Buckmaster, The quenching of deflagration waves, Combust. Flame 26 (1976) 151–162.
[3] J.D. Buckmaster, G.S.S. Ludford, in: Theory of Laminar Flames, Cambridge University Press, Cambridge, 1982, pp. 38–57.
[4] Y.D. Kim, M. Matalon, Propagation and extinction of a premixed flame in a stagnation-point flow, Combust. Flame 73 (1988) 303–313.
[5] I. Ishizuka, C.K. Law, An experimental study on extinction and stability of stretched premixed flames, in: Proceedings of the Nineteenth Symposium (International) on Combustion, The Combustion Institute, Pittsburgh, 1982, pp. 327–335.
[6] J. Sato, Effects of Lewis number on extinction behavior of premixed flames in a stagnation flow, in: Proceedings of the Nineteenth Symposium (International) on Combustion, The Combustion Institute, Pittsburgh, 1982, pp. 1541–1548.
[7] H. Tsuji, I. Yamaoka, Structure and extinction of near-limit flames in a stagnation flow, in: Proceedings of the Nineteenth Symposium (International) on Combustion, The Combustion Institute, Pittsburgh, 1982, pp. 1533–1540.
[8] C.L. Huang, C.P. Chiu, T.H. Lin, The influence of liquid fuel on the flame propagation of dilute sprays, J. Chin. Soc. Mech. Eng. 10 (1989) 333–343.
[9] C.C. Liu, T.H. Lin, The interaction between external and internal heat losses on the flame extinction of dilute sprays, Combust. Flame 85 (1991) 468–476.
[10] S.S. Hou, C.C. Liu, T.H. Lin, The influence of external heat transfer on flame extinction of dilute sprays, Int. J. Heat Mass Transfer 36 (7) (1993) 1867–1874.
[11] S.S. Hou, T.H. Lin, A theory on excess-enthalpy spray flame, Atomization and Sprays 9 (1999) 355–369.
[12] C.C. Liu, T.H. Lin, J.H. Tien, Extinction theory of stretched premixed flames by inert sprays, Combust. Sci. Technol. 91 (1993) 309–327.
[13] S.S. Hou, T.H. Lin, Extinction of stretched spray flames with nonunity Lewis numbers in a stagnation-point flow, in: Proceedings of the Twenty-Seventh Symposium (International) on Combustion, Pittsburgh, The Combustion Institute, 1998, pp. 2009–2015.
[14] T.H. Lin, C.K. Law, S.H. Chung, Theory of laminar flame propagation in off-stoichiometric dilute sprays, Int. J. Heat Mass Transfer 31 (5) (1988) 1023–1034.
[15] Williams, F.A., 1985. Combustion Theory, second ed., Benjamin Cummings, Menlo Park, CA, pp. 446–484.
[16] J.H. Tien, M. Matalon, Effect of swirl on strained premixed flames for mixtures with Lewis number distinct from unity, Combust. Sci. Technol. 87 (1993) 257–273.
[17] Z.H. Chen, T.H. Lin, S.H. Sohrab, Combustion of liquid fuel sprays in stagnation-point flow, Combust. Sci. Technol. 60 (1988) 63–77.
[18] C.C. Liu, Studies on flame extinction in two-phase combustible flows, Ph.D. thesis, National Cheng Kung University, Taiwan, ROC, 1992.
[19] C.C. Shu, R.H. Chen, C.C. Liu, T.H. Lin, Flow and flame characteristics of stagnation-point premixed flames influenced by water sprays, in: H.H. Chiu, N. Chigier (Eds.), Mechanics and Combustion of Droplets and Sprays, Begell House, 1995, pp. 376–386.
[20] R.H. Chen, M.C. Chen, J.T. Liu, T.H. Lin, Burning sprays of diesel fuel with azido compound in a stagnation-point two-phase flow, in: Proceedings of the Fourth International Conference on Technologies and Combustion for a Clean Environment, Lisbon, Portugal, 1997, pp. 161–166.